

Theoretical Calculations of Sea Surface Elevation Excess Kurtosis

A. V. Garmashov, A. S. Zapevalov *

Marine Hydrophysical Institute of RAS, Sevastopol, Russia

* e-mail: sezepter@mail.ru

Abstract

The excess kurtosis of sea surface elevation is a predictor of rogue waves. This paper verifies the dependencies of excess kurtosis on wave steepness ε and inverse wave age ζ , obtained for the JONSWAP wave spectrum. For verification, the paper uses data from *in situ* wave measurements conducted from a stationary oceanographic platform located in the coastal zone of the Black Sea. It is shown that in a real sea wave field, the excess kurtosis changes within significantly wider limits than those described by both model dependencies. The correlation coefficient between λ_4^E and ε is 0.06, and between λ_4^E and ζ is 0.05. The model dependence of λ_4^E on steepness ε is close to the linear regression constructed for wind waves, i. e., it allows describing only its average changes. The model dependence of excess kurtosis on inverse wave age overestimates its average values; the overestimation is approximately 0.1 and depends on ζ . Thus, the dependencies of the excess kurtosis of sea surface elevation on wave steepness and inverse wave age, constructed on the basis of the JONSWAP spectrum, do not allow describing the entire range of excess kurtosis changes in a real wave field. Rogue waves are observed in the sea when λ_4^E exceeds the threshold level of 0.6–0.7, while the maximum model values of excess kurtosis at the limiting Stokes wave steepness do not exceed the level of 0.3.

Keywords: wind wave modelling, excess kurtosis, surface wave spectrum, wave steepness, inverse wave age, Black Sea, JONSWAP spectrum, rogue waves

Acknowledgments: The work was carried out under state assignment FNNN-2024-0001 “Fundamental research of the processes determining the flows of matter and energy in the marine environment and at its borders, the state and evolution of the physical and biogeochemical structure of marine systems in modern conditions” and FNNN-2024-0014 “Fundamental studies of interaction processes in the sea-air system that form the physical state variability of the marine environment at various spatial and temporal scales”.

For citation: Garmashov, A.V. and Zapevalov, A.S., 2025. Theoretical Calculations of Sea Surface Elevation Excess Kurtosis. *Ecological Safety of Coastal and Shelf Zones of Sea*, (4), pp. 64–75.

© Garmashov A. V., Zapevalov A. S., 2025



This work is licensed under a Creative Commons Attribution-Non Commercial 4.0 International (CC BY-NC 4.0) License

Теоретические расчеты эксцесса возвышений морской поверхности

А. В. Гармашов, А. С. Запевалов *

Морской гидрофизический институт РАН, Севастополь, Россия

* e-mail: sevzepter@mail.ru

Аннотация

Эксцесс возвышений морской поверхности является предиктором возникновения аномально высоких волн. В работе верифицируются полученные для волнового спектра *JONSWAP* зависимости эксцесса от крутизны ε и от обратного возраста волн ζ . Для верификации используются данные прямых волновых измерений, проведенных со стационарной океанографической платформы, установленной в прибрежной зоне Черного моря. Показано, что в реальном поле морских волн эксцесс λ_4^E изменяется в значительно более широких пределах, чем предсказывается обеими модельными зависимостями. Коэффициент корреляции между λ_4^E и ε равен 0.06, между λ_4^E и ζ – 0.05. Модельная зависимость обратного возраста волн λ_4^E от крутизны ε близка к линейной регрессии, построенной для ветровых волн, то есть позволяет описать только его средние изменения. Модельная зависимость эксцесса от обратного возраста волн завышает его средние значения приблизительно на 0.1, причем завышение зависит от ζ . Таким образом, построенные на основе спектра *JONSWAP* зависимости эксцесса возвышений морской поверхности от крутизны волн и обратного возраста волн не позволяют описать весь диапазон изменчивости эксцесса в реальном волновом поле. Аномальные волны наблюдаются в море при превышении λ_4^E порогового уровня 0.6–0.7, тогда как максимальные модельные значения эксцесса при предельной крутизне волн Стокса не превышают уровень 0.3.

Ключевые слова: моделирование ветровых волн, эксцесс, спектр поверхностных волн, крутизна волн, обратный возраст волн, Черное море, спектр *JONSWAP*, аномальные волны

Благодарности: работа выполнена в рамках государственного задания ФГБУН ФИЦ МГИ по теме FNNN-2024-0001 «Фундаментальные исследования процессов, определяющих потоки вещества и энергии в морской среде и на ее границах, состояние и эволюцию физической и биогеохимической структуры морских систем в современных условиях» и FNNN-2024-0014 «Фундаментальные исследования процессов взаимодействия в системе океан-атмосфера, формирующих изменчивость физического состояния морской среды на различных пространственно-временных масштабах».

Для цитирования: Гармашов А. В., Запевалов А. С. Теоретические расчеты эксцесса возвышений морской поверхности // Экологическая безопасность прибрежной и шельфовой зон моря. 2025. № 4. С. 64–75. EDN VCOCEY.

Introduction

The number of global and regional spectral wave models of the sea surface has increased and the quality of forecasts produced by these models has improved [1]. Verification against *in situ* and remote sensing data demonstrates that these models represent significant wave height accurately [2–4].

A linear wave field obeys Gaussian statistics and, under the additional assumption of a narrow-band wave spectrum, the wave height distribution follows the Rayleigh distribution [5, 6]. Sea waves are a weakly nonlinear process whose cumulants deviate from zero values [7–10]. The deviation of the wave height distribution induced by nonlinearity is small for most of the distribution; however, it is significant for the tail of the distribution and is therefore of great importance for predicting the occurrence of rogue waves [11].

Rogue waves are typically characterized by the abnormality index (*AI*) which is the ratio of the maximum wave height recorded during the measurement period to the significant wave height. A wave is considered rogue if $AI > 2$ [12]. Studies conducted in various regions of the World Ocean have shown that *AI* statistically depends only on the excess kurtosis of sea surface elevation [13–15]. These studies suggest that excess kurtosis could be used to predict the probability of rogue waves occurring, which has led to the development of methods for calculating it based on spectral wave models [16–18]. The representation of excess kurtosis in the form of multidimensional integrals of wave spectra is used for these calculations [19, 20].

The study¹⁾ proposes simple parameterizations for the dependence of statistical moments of surface elevations on the wave field development stage. These parameterizations have various applications, including operational wave forecasting. They are derived under the same assumptions as those underpinning the kinetic equation in spectral wave models. However, the situations in which these parameterizations are applicable, as well as the feasibility of calculating excess kurtosis within spectral models, require further discussion.

This study aims to verify the relationship between excess kurtosis, wave steepness and inverse wave age, as obtained from the JONSWAP wave spectrum.

Methods and materials

Excess kurtosis. The higher order cumulants of a random variable serve as a measure of how much its distribution deviates from a Gaussian distribution. The fourth order cumulant, or excess kurtosis, is related to the statistical moments by the following expression:

$$\lambda_4 = \frac{\mu_4}{\mu_2^2} - 3,$$

where μ_2 , μ_4 are the central statistical moments of the second and fourth orders, respectively.

¹⁾ Janssen, P.A.E.M. and Bidlot, J.R., 2009. *On the Extension of the Freak Wave Warning System and its Verification*. ECMWF Technical Memoranda; 588. ECMWF, 42 p. <https://doi.org/10.21957/uf1sybog>

Studies [17, 19] developed an approach for calculating third and fourth order cumulants directly from known wave spectra. The wave spectrum derived from the Joint North Sea Wave Project (JONSWAP) remains the most widely used representation of the sea surface. The project was designed to investigate the generation and evolution of wind-driven waves in the North Sea [21, 22]. One of its key outcomes was the development of an empirical frequency-angular spectrum for the surface wave field. The two-dimensional JONSWAP frequency-angular spectrum takes the following form:

$$E(\omega, \theta) = 4\pi^2 \frac{\alpha g^2}{\omega^5} \left(\frac{\omega}{\omega_p} \right) \exp \left[-\frac{5}{4} \left(\frac{\omega}{\omega_p} \right)^2 \right] \gamma \exp \left[-\left(\frac{\omega}{\omega_p} - 1 \right)^2 / (2\sigma^2) \right] \Theta(\theta), \quad (1)$$

where ω is angular frequency; α is parameter that determines the wave energy; g is gravitational acceleration; γ and σ are parameters that determine the shape of the spectrum; $\Theta(\theta)$ is angular distribution function of wave energy; θ is azimuthal angle. Here and subsequently, index p indicates that the given parameter corresponds to the peak frequency of the wave spectrum.

Parameter σ has two fixed values: $\sigma = 0.07$ when the condition $\omega < \omega_p$ is satisfied and $\sigma = 0.09$ otherwise. Therefore, the one-dimensional spectrum depends on two parameters α and γ . The value of α , which determines the wave energy, is proportional to the square of the wave steepness ε :

$$\varepsilon = k_p \sqrt{\mu_2},$$

where k is the wave number. Accordingly, the steepness can be estimated by knowing the spectrum parameters (formula (1)). Parameters ω_p and k_p are related to each other by the dispersion relation for gravity waves in deep water, $\omega^2 = gk$. Parameter γ determines the excess in the spectral peak region relative to the Pierson – Moskowitz spectrum [23].

A two-parameter equation has been proposed for the JONSWAP spectrum based on the approach developed in [17, 19, 20], which relates the cumulants of sea surface elevations to the wave spectrum. This equation allows the excess kurtosis to be calculated ¹⁾:

$$\lambda_4^{SJ} = 12.6 \gamma^{-0.328} \varepsilon^2. \quad (2)$$

Here and thereafter, the superscript SJ indicates that the given parameter has been calculated for the JONSWAP spectrum. Equation (2) was derived for cases where the angular distribution function $\Theta(\theta)$ is specified in the following form:

$$\Theta(\theta) = \frac{1}{2} \beta \operatorname{sech}^2(\beta\theta), \quad (3)$$

where $\beta = \begin{cases} 261(\omega/\omega_p)^{1.3} & \text{at } 0.56 \leq \omega/\omega_p < 0.95, \\ 228(\omega/\omega_p)^{-1.3} & \text{at } 0.95 \leq \omega/\omega_p < 1.6, \\ 1.24 & \text{at } 1.6 < \omega/\omega_p. \end{cases} \quad (4)$

The mean direction of wave propagation is defined as the angle $\theta = 0$ in equation (3).

To calculate the dependence of excess kurtosis on the wave field development stage, a modified JONSWAP spectrum was employed in¹⁾ [24]. The parameters of this spectrum (also known as the Donelan spectrum) are explicit functions of the inverse wave age:

$$\zeta = U_{10} / C_p,$$

where U_{10} is wind speed at a height of 10 m; C_p is phase speed. Higher values of ζ correspond to an earlier stage of wave development. A fully developed wind sea corresponds to $\zeta_0 = 0.83$; for $\zeta > \zeta_0$, the waves are considered wind-driven, whereas for $\zeta < \zeta_0$, they are classified as swell.

The Donelan spectrum has the form

$$E_D(\omega, \theta) = 4\pi^2 \frac{\alpha_D g^2}{\omega^5} \left(\frac{\omega}{\omega_p} \right) \exp \left[- \left(\frac{\omega}{\omega_p} \right)^2 \right] \gamma_D \exp \left[- \left(\frac{\omega}{\omega_p} - 1 \right)^2 / (2\sigma^2) \right] \Theta(\theta), \quad (5)$$

where

$$\alpha_D = 0.006 \zeta^{0.55} \quad \text{at } 0.83 < \zeta < 5,$$

$$\sigma_D = 0.08 (1 + 4/\zeta^3) \quad \text{at } 0.83 < \zeta < 5,$$

$$\gamma_D = \begin{cases} 1.7 & \text{at } 0.83 < \zeta < 1, \\ 1.7 + 6.0 \lg \zeta & \text{at } 1 < \zeta < 5. \end{cases}$$

The following dependence¹⁾ has been obtained for the Donelan spectrum and the angular distribution function in the form of equations (3) and (4):

$$\lambda_4^{SD} = 0.04 + 0.082 \zeta^{0.87}, \quad (6)$$

where the superscript *SD* indicates that the excess kurtosis has been calculated using the Donelan spectrum. The accuracy of model (6) largely depends on how well wave spectrum (5) captures the dependence on inverse wave age. A previous analysis compared wind wave spectra with the Donelan spectrum based on measurements from an oceanographic platform under conditions of variable wind speed and strong swell [25]. This analysis showed that, on average, the dependencies of spectral parameters on wave age obtained under different conditions align with the formulas derived for a pure wind sea under stable wind conditions.

Data and measurement conditions. We use data from wave measurements conducted on the stationary oceanographic platform operated by Marine Hydrophysical Institute of RAS to verify the relationships describing the dependence of excess kurtosis on wave steepness and inverse wave age. The platform is located in the coastal zone of the Black Sea, off the southern coast of Crimea. The minimum distance from the platform to the shoreline is approximately 600 m, with the water depth at the site around 30 m. Wave measurements were performed using a resistive wave gauge consisting of a nichrome wire wound with constant pitch on a supporting cable. Wind speed was measured with a cup anemometer [26].

Wave measurements were conducted from May 2018 to January 2019. For the analysis, continuous records were divided into 20-minute segments and statistical characteristics of waves and wind speed were calculated for each segment. The conditions for conducting wave measurements on the stationary oceanographic platform are described in [9, 10]. The wind regime in the vicinity of the platform was analysed in [27].

During the measurement period, the significant wave height H_s reached 2.3 m and the mean wind speed at 10 m height (U_{10}) reached 26 m/s. Wave steepness ε and inverse wave age ζ ranged from $0 < \varepsilon < 0.14$ and $0 < \zeta < 6.3$, respectively. Value $\zeta = 0$ corresponds to wind speeds below the anemometer startup threshold. High values of ζ were observed under short-fetch conditions, which corresponded to onshore winds.

Results and discussion

Two components of nonlinearity that cause deviations from the Gaussian distribution in a random wave field have been identified [17]. The first component, arising from nonlinear inter-wave interactions, is referred to as “dynamic” as it is associated with the evolution of the wave field. The second component is related to the presence of bound waves in the field. The term “bound components” includes Stokes wave harmonics, as well as all harmonics generated by nonlinear inter-wave interactions that do not satisfy the linear dispersion relation¹⁾.

In the general case of a broadband random wave field, the dynamic contribution to excess kurtosis is small in absolute value and negligible compared to the contribution of bound components [17]. We can compare relation (6) obtained within the spectral wave model framework, with the dependence of excess kurtosis on wave steepness, as obtained within the second order nonlinear model. In this model, the deviation from Gaussian distribution is determined by bound components [28].

The second order nonlinear model is built up from a combination of linear and nonlinear elements:

$$\eta(x, t) = \eta_L(x, t) + \eta_N(x, t),$$

where η is sea surface elevation; x is spatial coordinate; t is time;

$$\begin{aligned} \eta_L(x, t) &= \sum_{n=1}^{\infty} a_n \cos \psi_n, \\ \eta_N(x, t) &= \sum_{m=1}^{\infty} \sum_{n=1}^{\infty} \left\{ a_n a_n \left[B_{mn}^- \cos(\psi_m - \psi_n) + B_{mn}^+ \cos(\psi_m + \psi_n) \right] \right\}, \end{aligned}$$

$\psi_n = k_n x - \omega_n t + \varphi_n$, φ_n is the phase; B_{mn}^- and B_{mn}^+ are second order transfer functions. Functions B_{mn}^- and B_{mn}^+ are derived from the Laplace equation for the velocity potential, subject to nonlinear boundary conditions. The model includes second order bound waves arising from interactions of free wave components.

According to the second order nonlinear model, excess kurtosis is related to wave steepness through the equation provided in [28].

$$\lambda_4^N = 12 \varepsilon^2 + O(\varepsilon^4). \quad (7)$$

Unlike relation (7), dependence (2) does not assume a one-to-one correspondence between excess kurtosis and wave steepness. When the wave field approaches a fully developed state, the average value of $\gamma \approx 1.7$; higher values of γ correspond to earlier stages of development. Within the observed range of γ , the inequality $\lambda_4^N > \lambda_4^{SJ}$ holds. This discrepancy increases with increasing γ .

Fig. 1 shows the dependence of excess kurtosis on wave steepness for wind waves, as determined from measurements in the coastal zone of the Black Sea, as well as theoretical dependencies (2) and (7). The dependencies $\lambda_4^N = \lambda_4^{SJ}(\varepsilon)$ were constructed for two values of the parameter γ : 1.7 and 3.3. As evident from the figure, the discrepancies between the theoretical dependencies are considerably smaller than the scatter in the measured excess kurtosis values. Fig. 1 also presents the linear regression:

$$\lambda_4^E = 0.94 \varepsilon + 0.01 \pm 0.21 \quad (8)$$

and the regression in the form $\lambda_4^E = \alpha^E \varepsilon^2$. Coefficient α^E is 19.5.

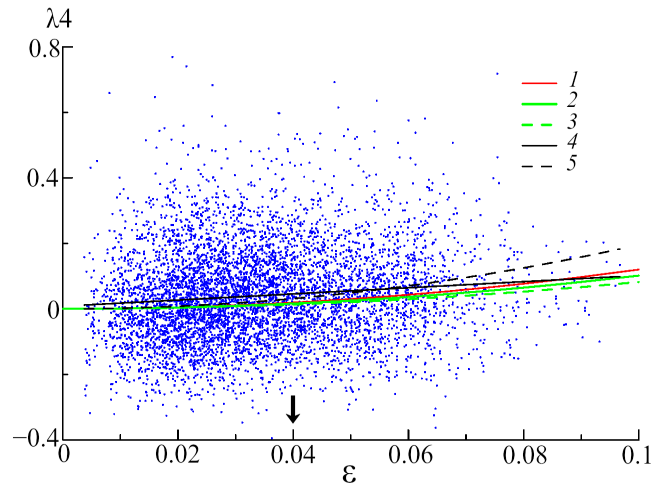


Fig. 1. Dependency of excess kurtosis λ_4 on steepness ε . The dots are experimental data; curve 1 is dependency (7), curves 2 and 3 are dependencies (2) obtained at $\gamma = 1.7$ and $\gamma = 3.3$; curve 4 is linear regression (8); curve 5 is regression in the form of $\lambda_4^E = \alpha^E \varepsilon^2$. The arrow shows the steepness calculated for the Pierson–Moskowitz spectrum

The fully developed wind sea spectrum is typically represented by the Pierson – Moskowitz spectrum [23]. The characteristic steepness value for this spectrum $\varepsilon_{PM} = 0.04$ is shown by the arrow in Fig. 1.

The correlation coefficient between λ_4^E and ε is 0.06. The absence of significant correlation between excess kurtosis and wave steepness, as determined by *in situ* measurements, is consistent with the results of laboratory experiments conducted in a wind wave flume [29, 30]. These experiments led to the conclusion that cumulants up to the eighth order (inclusive) depend on steepness, with the notable exception of excess kurtosis, for which no clear dependence on ε was identified.

As Fig. 1 shows, the changes in excess kurtosis calculated using models (2) and (7) when steepness varies from 0 to 0.1 are much smaller than the observed changes in excess kurtosis in a real wave field. At the same time, the model dependencies closely resemble the linear and quadratic regression dependencies and adequately describe the average state of the sea surface.

Fig. 2 shows the experimental and model dependencies of excess kurtosis λ_4 on inverse wave age ζ . Similar to the $\lambda_4^E = \lambda_4^E(\varepsilon)$ dependence, the $\lambda_4^E = \lambda_4^E(\zeta)$ dependence is characterized by a large scatter in the values of λ_4^E . The correlation coefficient between λ_4^E and ζ is 0.05. A comparison of dependence (6) with the linear regression described by the equation

$$\lambda_4^{ER} = 0.001 + 0.0288 \zeta \pm 0.20, \quad (9)$$

shows that the model estimates of excess kurtosis exceed consistently the average values obtained through experimentation. Overestimation $\lambda_4^{SD}(\zeta) - \lambda_4^{ER}(\zeta)$ increases from 0.085 at $\zeta = 0.83$ to 0.18 at $\zeta = 3.3$.

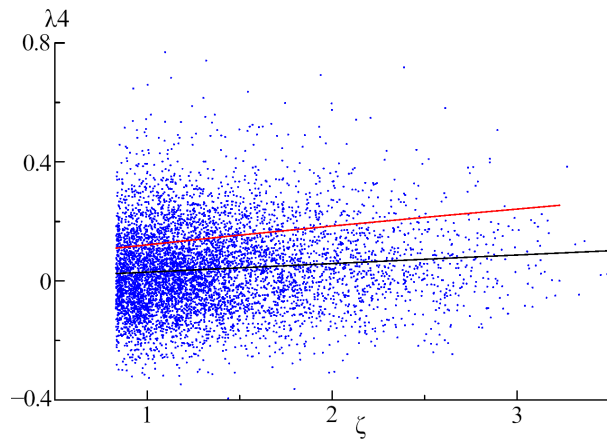


Fig. 2. Dependency of excess kurtosis λ_4 on inverse wave age ζ . The dots are experimental data; the red line is dependency (6); the black line is linear regression (9)

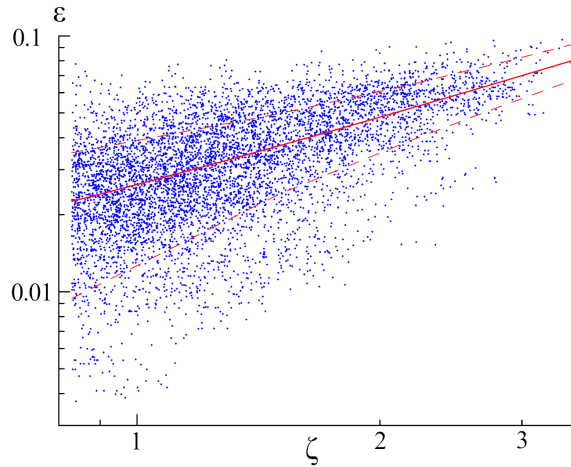


Fig. 3. Dependency of steepness ε on inverse wave age ζ . The dots are experimental data; the solid line is linear regression (10); the dashed lines show deviations ± 0.013

Rogue waves occur when excess kurtosis values exceed a critical level estimated to lie within the range of 0.6–0.7. However, as can be seen from Figs. 1 and 2, the model values of excess kurtosis never exceed 0.3, meaning they cannot be used to forecast the occurrence of rogue waves.

Another drawback of dependencies (2) and (7) should be noted. The excess kurtosis values obtained using these are always positive, which does not correspond with *in situ* measurement results.

Dependence (6), as proposed in¹⁾ relies on the assumption that specifying the inverse wave age alone provides a sufficiently accurate description of the spectrum and integral parameters of the wave field, including variations in steepness across different stages of wave development. However, the validity of this assumption depends on the accuracy and clarity of the parameterization used for the Donegal spectrum.

Fig. 3 shows the dependence of wave steepness on inverse wave age, as determined from wave measurements. As evident from the figure, the relationship between ε and ζ for wind waves is stochastic. Cases, where $\zeta > 3.5$, are rare and have therefore been excluded from the present study. At the same value of ζ , the values of ε can differ by an order of magnitude. For the dataset analyzed in this study, the correlation coefficient between ε and ζ is 0.63. The linear regression equation takes the form

$$\varepsilon = 0.022 \zeta + 0.004 \pm 0.013. \quad (10)$$

Conclusion

The rogue wave index depends statistically only on the excess kurtosis of sea surface elevations. This relationship suggests the potential for using excess kurtosis to predict the probability of rogue waves occurrence and has stimulated the development of computational methods based on various models. However, verification of the predicted dependence of excess kurtosis on wave steepness ε and inverse wave age ζ , as derived from the JONSWAP spectrum, demonstrates that these dependencies cannot describe the full range of excess kurtosis variations in a real wave field. Negligible correlation is observed between excess kurtosis and parameters ε and ζ , which makes it impossible to use these dependencies to forecast rogue wave occurrence. Additionally, a significant discrepancy exists between dependencies (2) and (7) and the observational data: the excess kurtosis values calculated using these dependencies are invariably positive, whereas negative values are frequently observed in field measurements.

REFERENCES

1. Grigorieva, V.G., Gulev, S.K. and Sharmer, V.D., 2020. Validating Ocean Wind Wave Global Hindcast with Visual Observations from VOS. *Oceanology*, 60(1), pp. 9–19. <https://doi.org/10.1134/S0001437020010130>
2. Mikhailichenko, S.Yu., Garmashov, A.V. and Fomin, V.V., 2016. Verification of the Swan Wind Waves Model by Observations on the Stationary Oceanographic Platform of the Black Sea Hydrophysical Polygon of RAS. *Ecological Safety of Coastal and Shelf Zones of Sea*, (2), pp. 52–57 (in Russian).
3. Stopa, J.E. and Cheung, K.F., 2014. Intercomparison of Wind and Wave Data from the ECMWF Reanalysis Interim and the NCEP Climate Forecast System Reanalysis. *Ocean Model*, 75, pp. 65–83. <https://doi.org/10.1016/j.ocemod.2013.12.006>
4. Stopa, J.E., Arduin, F., Bababin, A.V. and Zieger, S., 2016. Comparison and Validation of Physical Wave Parameterizations in Spectral Wave Models. *Ocean Model*, 103, pp. 2–17. <https://doi.org/10.1016/j.ocemod.2015.09.003>
5. Longuet-Higgins, M.S., 1957. The Statistical Analysis of a Random, Moving Surface. *Philosophical Transactions of the Royal Society of London. Series A, Mathematical and Physical Sciences*, 249(966), pp. 321–387. <https://doi.org/10.1098/rsta.1957.0002>
6. Goda, Y., 2000. *Random Seas and Design of Maritime Structures*. Singapore: World Scientific Publishing Co., 443 p.
7. Babanin, A.V. and Polnikov, V.G., 1995. On Non-Gaussian Wind Waves. *Physical Oceanography*, 6(3), pp. 241–245. <https://doi.org/10.1007/BF02197522>
8. Guedes Soares, C., Cherneva, Z. and Antão E.M., 2004. Steepness and Asymmetry of the Largest Waves in Storm Sea states. *Ocean Engineering*, 31(8-9), pp. 1147–1167. <https://doi.org/10.1016/J.OCEANENG.2003.10.014>
9. Zapevalov, A.S. and Garmashov, A.V., 2021. Skewness and Kurtosis of the Surface Wave in the Coastal Zone of the Black Sea. *Physical Oceanography*, 28(4), pp. 414–425. <https://doi.org/10.22449/1573-160X-2021-4-414-425>
10. Zapevalov, A.S. and Garmashov, A.V., 2022. The Appearance of Negative Values of the Skewness of Sea-Surface Waves. *Izvestiya, Atmospheric and Oceanic Physics*, 58(3), pp. 263–269. <https://doi.org/10.1134/s0001433822030136>
11. Stansell, P., 2004. Distributions of Freak Wave Heights Measured in the North Sea. *Applied Ocean Research*, 26(1-2), pp. 35–48. <https://doi.org/10.1016/j.apor.2004.01.004>

12. Annenkov, S.Y. and Shrira, V.I., 2013. Large-Time Evolution of Statistical Moments of Wind-Wave Fields. *Journal of Fluid Mechanics*, 726, pp. 517–546. <https://doi.org/10.1017/jfm.2013.243>
13. Kharif, C., Pelinovsky, E. and Slunyaev, A., 2009. *Rogue Waves in the Ocean*. Advances in Geophysical and Environmental Mechanics and Mathematics. Berlin; Heidelberg: Springer, 216 p. <https://doi.org/10.1007/978-3-540-88419-4>
14. Tomita, H. and Kawamura, T., 2000. Statistical Analysis and Inference from the In Situ Data of the Sea of Japan with Reference to Abnormal and/or Freak Waves. In: ISOPE, 2000. *Proceedings of 10th ISOPE Conference. May 28 – June 2, 2000. Seattle, USA*. The International Society of Offshore and Polar Engineers, ISOPE-I-00-232.
15. Ivanov, V.A., Dulov, V.A., Kuznetsov, S.Yu., Dotsenko, S.F., Shokurov, M.V., Saprykina, Y.V., Malinovsky, V.V. and Polnikov, V.G., 2012. Risk Assessment of Encountering Killer Waves in the Black Sea. *Geography, Environment, Sustainability*, 5(1), pp. 84–111. <https://doi.org/10.24057/2071-9388-2012-5-1-84-111>
16. Zapevalov, A.S. and Garmashov, A.V., 2022. Probability of the Appearance of Abnormal Waves in the Coastal Zone of the Black Sea at the Southern Coast of Crimea. *Ecological Safety of the Coastal and Shelf Zones of the Sea*, (3), pp. 6–15.
17. Annenkov, S.Y. and Shrira, V.I., 2009. Evolution of Kurtosis for Wind Waves. *Geophysical Research Letters*, 36(13), L13603. <https://doi.org/10.1029/2009GL038613>
18. Annenkov, S.Y. and Shrira, V.I., 2013. Large-Time Evolution of Statistical Moments of Wind-Wave Fields. *Journal of Fluid Mechanics*, Vol. 726, pp. 517–546. <https://doi.org/10.1017/jfm.2013.243>
19. Mori, N., Onorato, M. and Janssen, P.A.E.M., 2011. On the Estimation of the Kurtosis in Directional Sea States for Freak Wave Forecasting. *Journal of Physical Oceanography*, 41(8), pp. 1484–1497. <https://doi.org/10.1175/2011JPO4542.1>
20. Janssen, P.A.E.M., 2003. Nonlinear Four-Wave Interactions and Freak Waves. *Journal of Physical Oceanography*, 33(4), pp. 863–884. [https://doi.org/10.1175/1520-0485\(2003\)33<863:NFIAFW>2.0.CO;2](https://doi.org/10.1175/1520-0485(2003)33<863:NFIAFW>2.0.CO;2)
21. Annenkov, S.Y. and Shrira, V.I., 2014. Evaluation of Skewness and Kurtosis of Wind Waves Parameterized by JONSWAP Spectra. *Journal of Physical Oceanography*, 44(6), pp. 1582–1594. <https://doi.org/10.1175/JPO-D-13-0218.1>
22. Hasselmann, K., Barnett, T.P., Bouws, E., Carlson, H., Cartwright, D.E., Enke, K., Ewing, J.A., Gienapp, H., Hasselmann, D.E. [et al.], 1973. Measurements of Wind-Wave Growth and Swell Decay During the Joint North Sea Wave Project (JONSWAP). *Ergänzungsheft zur Deutschen Hydrographischen Zeitschrift Reihe A*(8), (12), 95 p.
23. Young, I.R., 1999. *Wind Generated Ocean Waves*. Amsterdam: Elsevier, 287 p.
24. Pierson, W.I. and Moskovitz, L., 1964. A Proposed Spectral Form for Fully Developed Wind Seas Based on the Similarity Theory of S. A. Kitaigorodskii. *Journal of Geophysical Research*, 69(24), pp. 5181–5190. <https://doi.org/10.1029/JZ069i024p05181>
25. Donelan, M.A., Hamilton, J. and Hui, W.H., 1985. Directional Spectra of Wind-Generated Waves. *Philosophical Transactions of the Royal Society of London. Series A, Mathematical and Physical Sciences*, 315(1534), pp. 509–562. <https://doi.org/10.1098/rsta.1985.0054>
26. Zapevalov, A.S., Dulov, V.A., Bolshakov, A.N., Smolov, V.E., Mostsipan, T.N. and Pokazeev, K.V., 2003. [On Spectral Characteristics of Wind Waves in the Coastal Area of the Black Sea]. In: Yu. D. Chashechkin and V. G. Baydulov, eds., 2003. *Fluxes and Structures in Fluids: Proceedings of the International Conference, 23–26 June 2003, Saint Petersburg*. Moscow, pp. 169–172 (in Russian).

27. Toloknov, Yu.N. and Korovushkin, A.I., 2010. The System of Collecting Hydrometeorological Information. In: MHI, 2010. *Monitoring Systems of Environment*. Sevastopol: ECOSI-Gidrofizika. Iss. 13, pp. 50–53 (in Russian).
28. Solov'ev, Y.P. and Ivanov, V.A., 2007. Preliminary Results of Measurements of Atmospheric Turbulence over the Sea. *Physical Oceanography*, 17(3), pp. 154–172. <https://doi.org/10.1007/s11110-007-0013-9>
29. Tayfun, M.A. and Alkhalidi, M.A., 2016. Distribution of Surface Elevations in Nonlinear Seas. In: OTC, 2016. *Proceedings of Offshore Technology Conference. Kuala Lumpur, Malaysia, 22–25 March 2016*. pp. 1274–1287. <https://doi.org/10.4043/26436-MS>
30. Huang, N. and Long, S., 1980. An Experimental Study of the Surface Elevation Probability Distribution and Statistics of Wind-Generated Waves. *Journal of Fluid Mechanics*, 101(1), pp. 179–200. <https://doi.org/10.1017/S0022112080001590>

Submitted 15.02.2025; accepted after review 23.06.2025;
revised 17.09.2025; published 30.12.2025

About the authors:

Anton V. Garmashov, Senior Research Associate, Marine Hydrophysical Institute of RAS (2 Kapitanskaya St., Sevastopol, 299011, Russian Federation), PhD (Geogr.), **Scopus Author ID: 54924806400**, **ResearcherID: P4155-2017**, ant.gar@mail.ru

Aleksandr S. Zapevalov, Chief Research Associate, Marine Hydrophysical Institute of RAS (2 Kapitanskaya St., Sevastopol, 299011, Russian Federation), DSc (Phys.-Math.), **ResearcherID: V-7880-2017**, **Scopus Author ID: 7004433476**, **ORCID ID: 0000-0001-9942-2796**, sevzepter@mail.ru

Contribution of the authors:

Anton V. Garmashov – collection of in situ measurement data, its systematisation, processing and analysis, analysis of literature sources

Aleksandr S. Zapevalov – problem statement, processing, analysis and description of the study results, preparation of the article text and graphic materials

All the authors have read and approved the final manuscript.